International Journal of Mass Spectrometry 291 (2010) 145–151

Contents lists available at ScienceDirect

International Journal of Mass Spectrometry

journal homepage: www.elsevier.com/locate/ijms

Effectiveness of platinum particle deposition on silicon surfaces for surface-assisted laser desorption/ionization mass spectrometry of peptides

Teruyuki Yao, Hideya Kawasaki, Takehiro Watanabe, Ryuichi Arakawa *

Department of Applied Chemistry, Kansai University, 3-3-35 Yamate-cho, Suita-shi, Osaka 564-8680, Japan

ARTICLE INFO

Article history:
Received 24 November 2009
Received in revised form 19 January 2010
Accepted 2 February 2010
Available online 6 February 2010

Keywords:
SALDI-MS
Small organic molecules
Pt nanoparticles
Galvanic displacement on silicon
Charge separation

ABSTRACT

One of the problems associated with surface-assisted laser desorption/ionization mass spectrometry (SALDI-MS) using metal nanoparticles is that peptide analytes are characterized by alkali metal ion adducts even though in the presence of an excess proton source of trifluoroacetic acid in the mass spectra, and their alkali metal ion adducts are often observed in the low peak intensity. In this study, to improve the detection of the proton adduct form of the peptides, the effectiveness of platinum (Pt) particle deposition on a silicon plate for SALDI-MS was examined using the following different Pt-deposited silicon substrates: (1) Pt galvanic deposition (PGDS), (2) Pt particles deposited by suspension deposition on silicon, (3) evaporated Pt on oxidized silicon, and (4) evaporated Pt on bare silicon. Among these substrates, the PGDS plate exhibited the dominant proton adduct form of peptides in the SALDI mass spectra. In addition to platinum deposition, we attempted to employ palladium galvanic deposition as a SALDI-MS substrate, but it was found to lead mainly to the Na^+ and K^+ forms of the molecular ion. We propose that UV laser radiation-mediated surface-localized positive charges generated by effective charge separation (electron and hole) in the PGDS are important for the production of the proton adduct forms of peptides. Gly-Gly-Tyr-Arg, caffeine, raffinose, and β-cyclodextrin were used as examples to demonstrate the feasibility of PGDS as a matrix-free method for LDI-MS. It was possible to detect these small molecules with SALDI-MS using PGDS; however, the detection sensitivity of these small molecules remains an unresolved issue.

1. Introduction

Matrix-assisted laser desorption/ionization time-of-flight mass spectrometry (MALDI-MS) with the use of conventional organic matrices has been extensively applied to the field of life sciences [1–7]. However, matrix ion interface and detector saturation are inevitable for the low mass molecules in MALDI-TOF-MS, which makes the characterization of small molecules obscure and difficult. As an organic matrix-free approach, surface-assisted laser desorption/ionization (SALDI) has emerged; this technique involves the use of substrate materials or particles, including carbon materials [8–10], metal oxides [11,12], and metallic particles [13,14], as LDI matrices. This technique was originally inspired by the early work of Tanaka et al., which used cobalt particles in a glycerol matrix [15]. Sunner et al. introduced the SALDI technique, using graphite particles in a liquid matrix [8]. More recently, nanomaterials without the use of liquid matrices, such as glycerol, have been adopted using carbon nanotubes (CNT) [16], ZnO [17], TiO_2 [18,19], Fe_2O_3/TiO_2 [20], Pt [21], and Au [22–26] and Ag [27,28] nanoparticles, including desorption/ionization from porous silicon (DIOS) [29,14,30], metal-coated porous alumina [31], and germanium dots [32]. One of the most important features of SALDI is its absence of matrix interferences in the low mass region in contrast to MALDI, and hence, it extends the observable mass range of small biomolecules to below 500 *m/z* [33]. Thus, the development of both MALDI and SALDI is important to respond to increasing demands for high throughput methods in drug discovery and biotechnology, as well as for the analysis of complex mixtures in high salt matrices and buffers over the entire mass range.

In previous studies, we reported on SALDI-MS using various metal nanoparticles such as Pt, Au, Ag, and Cu for peptides [34], where the use of Pt nanoparticles resulted in superior SALDI-MS performance of angiotensin I. One of the problems associated with SALDI-MS using these metal nanoparticles was that analytes were characterized by alkali metal ion adducts formed in the presence of an excess trifluoroacetic acid (TFA) proton source, and their alkali metal ion adducts were observed in the low peak intensity and poor resolution [34]. In SALDI-MS, using these metal nanoparticles, a citrate buffer provided an effective proton source to yield the proton adduct form, and the intensity of the mass spectra of the peptides

* Corresponding author. Tel.: +81 6 6368 5647; fax: +81 6 6339 4026.
E-mail address: arak@kansai-u.ac.jp (R. Arakawa).

1387-3806/$ – see front matter © 2010 Elsevier B.V. All rights reserved.
doi:10.1016/j.ijms.2010.02.001

was improved due to the reduced adduction of the chelated alkali cations [34,35]. However, the use of citrate buffer yielded strong molecular ion peaks of citrate in the low mass region, which could frequently be observed below 500 m/z. This results in loss of the advantages of the matrix-free approach in SALDI-MS. In another approach, the surface modification of metal nanoparticles such as 4-aminothiophenol resulted in an increase in the protonated ions of peptides [24].

More recently, the generation of proton adduct ions of peptides from silicon substrates in desorption/ionization mass spectrometry (DIOS-MS) was investigated, and a new model for protonated ion generation of peptides was proposed [39,40]. In this model, the electronic excitation of an activated silicon substrate to form free electron/hole pairs and their subsequent relaxation result in the formation of trapped positive charges of holes in the near surface, causing an increase in the acidity of the Si–OH groups. As a result, proton transfer from the Si–OH groups to the analyte molecules is enhanced, and finally, the thermally activated analyte ions dissociate from the surface. The use of hydrogenated amorphous silicon as the SALDI plate results in a near total loss of SALDI performance, while amorphous silicon provides an excellent high-sensitivity substrate [40].

According to this model, it is expected that the deposition of platinum nanoparticles on an n-type silicon surface, corresponding to the n-Si/Pt Schottky barrier, would accelerate the near-surface hole-trapping events because of a reduction in the recombination process of the electron/hole pairs, resulting in an increase in the number of protonated ions of peptides. Therefore, in this study, we investigated platinum galvanic deposition on silicon for SALDI-MS. The plate was simply prepared by immersing an n-type silicon substrate into an HF aqueous solution containing Pt salt, where the direct growth of Pt particles on the bare silicon surface proceeded spontaneously in the HF aqueous solution through an electroless galvanic reaction between the aqueous solution of Pt salt and the bare silicon substrate [36–38]. To explore the conditions of the plate utilized for SALDI-MS, the SALDI performance was examined for the following different types of Pt-deposited silicons: (1) galvanic deposition of Pt on bare silicon (n-Si/Pt contact), (2) evaporated Pt on bare silicon (n-Si/Pt contact), (3) evaporated Pt on oxidized silicon (n-Si/SiO_2/Pt contact), and (4) Pt particle deposition from the suspension. We found that the proton adduct form of the peptides was dominant in the SALDI mass spectra using galvanic deposition of Pt on bare silicon and evaporated Pt on bare silicon. The generation mechanism to yield the proton adduct form of the peptides will be discussed using the UV radiation-mediated surface-localized positive charges generated by charge separation (electron and hole) in Pt particles on a bare silicon surface.

2. Experimental

2.1. Materials and reagents

Acetone, methanol, ethanol, 46% hydrofluoric acid, trifluoroacetic acid (TFA), hexachloroplatinum (IV) acid ($H_2PtCl_6{\cdot}7H_2O$), palladium(II) chloride, angiotensin II, caffeine, raffinose, β-cyclodextrin, vitamin C, and aspirin were purchased from Wako Pure Chemicals (Osaka, Japan), and Gly-Gly-Tyr-Arg (GGYR) was purchased from Peptide Institute, Inc. (Osaka, Japan). Silicon wafers (⟨1 0 0⟩, n-type, 0.012–0.02 Ω cm) were purchased from Sumco Corporation (Tokyo, Japan).

2.2. Platinum galvanic deposition on silicon (PGDS)

The Si wafers were cut into 1.5 cm × 1.5 cm squares, sonicated in acetone and methanol for 10 min each, and etched with 46% hydrofluoric acid for 20 min. The electroless displacement deposition of these metals was carried out by immersing the n-Si substrates in a 1 mM metal-salt (H_2PtCl_6 or $PdCl_2$) solution containing 5 M hydrofluoric acid. After immersion, these substrates were washed with water and preserved in ethanol.

2.3. Platinum evaporation coating on silicon

In this study, two different substrate preparation methods were used; these methods will be hereafter referred to as methods A and B. In method A, the oxidation of the Si substrates was performed by irradiating them with UV–ozone for 30 min. Evaporated Pt with a thickness of 20 nm was prepared on this silicon substrate (plate A, n-Si/SiO_2/Pt contact). In method B, the Si substrate was immersed in 46% hydrofluoric acid solution for 20 min to remove the oxidation layer from the Si surface, and then, the evaporated Pt with a thickness of 20 nm was prepared on this silicon substrate (plate B, n-Si/Pt contact).

2.4. Platinum powder

The Pt source $H_2PtCl_6{\cdot}7H_2O$ (1 g, 1.95 mmol) was dissolved in 150 cm^3 of deionized water. Under vigorous stirring, the reductant ($NaBH_4$, 380 mg, 10 mmol) was gradually introduced into this aqueous solution [21]. The black dispersion was continuously stirred for several hours. Black precipitates consisting of spherical Pt nanoparticles were then collected by centrifugation at 4000 rpm for 10 min. The black powder obtained here was washed with pure water several times in order to eliminate free ions, such as Na^+ or unreduced $PtCl_6^{2-}$, BO_3^{2-}. The Pt powder was then dried in vacuum for >12 h at room temperature. The dried powder was kept in ambient atmosphere in a glass tube.

2.5. SALDI-TOF-MS

The prepared silicon plate with the deposition of Pt was fixed to a stainless-steel sample plate with conductive carbon double-sided tape. The sample solution containing 0.5 μL of a cationization agent (0.1% TFA) was spotted with this substrate and dried under reduced pressure. In the case using the Pt powder, the two-layer sample preparation method was employed for SALDI-MS: the first step was the spotting of the Pt powder suspension (1 μL, 15 mg/mL), which was prepared by dispersing Pt powder in pure water with ultrasonication for 5 min on a stainless-steel plate followed by drying; the second step was the typical deposition of a 0.5 μL sample solution on the plate. The SALDI mass spectra were obtained in the linear mode, using an AXIMA CFR TOF-MS (Shimadzu, Kyoto, Japan) fitted with a pulsed nitrogen laser (337 nm). 100 laser shots were used to acquire the mass spectra. The analyte ions were accelerated at 20 kV under delayed extraction conditions.

2.6. Atomic force microscope (AFM)

AFM images of the substrates were acquired at 25 ± 2 °C in tapping modes on a NanoScope IIIa (Veeco). The AFM images were obtained at a scan rate of 0.5 Hz using silicon tips with a nominal spring constant of 42 N m^{-1} in air.

2.7. Scanning electron microscope (SEM)

An SEM (JEOL JSM-6700) was used to observe surface structures at an accelerating voltage of 5.0 kV.

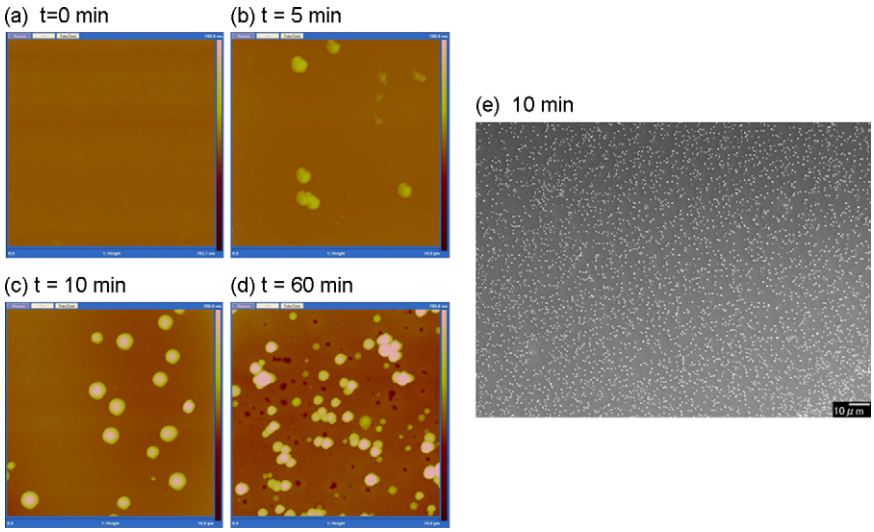

Fig. 1. AFM image of the PGDS plate as a function of immersing times (t/min) of (a) 0 min, (b) 5 min, (c) 10 min, and (d) 60 min. (e) SEM image at an immersing time of 10 min.

3. Results and discussion

3.1. Galvanic deposition of Pt on silicon from aqueous HF solutions

Platinum galvanic deposition on silicon (PGDS) occurs by a local cell mechanism, which consists of a local cathode deposition of Pt particles with the injection of holes into the valence band of the n-Si, and the local anode dissolution of silicon by the injected holes and HF [36–38]. Thus, the reduction of Pt ions and silicon etching occur simultaneously at the silicon surface in the absence of externally applied potentials. Fig. 1 shows the typical AFM images of the PGDS plate as a function of immersing times (t/min). At $t = 0$ (i.e., original silicon), a very flat surface with root-mean-square (rms) roughness of less than 0.2 nm characterizes the flatness of the original silicon sample. After the bare silicon substrate was immersed into Pt salt solutions containing HF, fine Pt particles were deposited on the silicon substrate. A small number of Pt particles with a few hundred nanometers in size appeared at $t = 5$ min (0.5×10^5/mm^2). The particle density increased to 1.5×10^5/mm^2 at 10 min. The height and the width of the metal particles were in the range of 100–400 nm and 200–1000 nm at $t = 10$ min, respectively. At $t = 60$ min, the particle density of Pt particles increased to 8×10^5/mm^2. The size of the metal particles remained basically unchanged, despite the longer deposition time. The observed SEM image at $t = 10$ min is also shown in Fig. 1e. Fine Pt particles deposited on the silicon substrate were observed. It is also worth noting that prolonged deposition time favors particle agglomeration; this fact is in agreement with other reported data [36]. The expanded AFM image shows that the surface roughness around the Pt particles increases to approximately 20 nm with respect to the original surface (not shown), which may have originated from the dissolution of silicon as a silicon hexafluoride ion [36–38]. The black spots in the AFM image at $t = 60$ min indicate holes on the silicon surface; however, the origin of the black spots was not clarified by investigations performed in the present study.

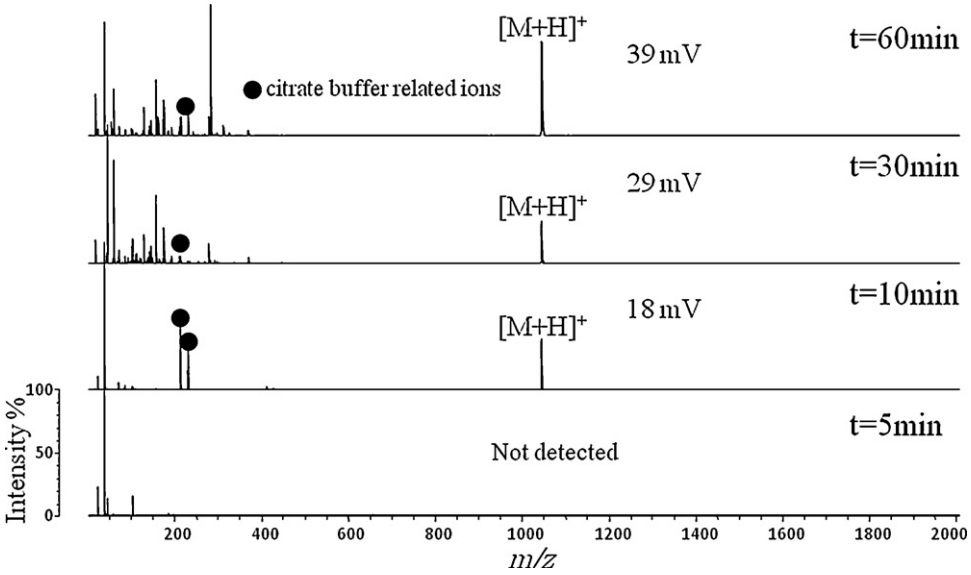

Fig. 2. SALDI mass spectra of angiotensin II (5 pmol) obtained using the PGDS plate with immersing times of 5, 10, 30, and 60 min in a positive ion mode. The peak intensity is denoted by a unit of mV in the figure.

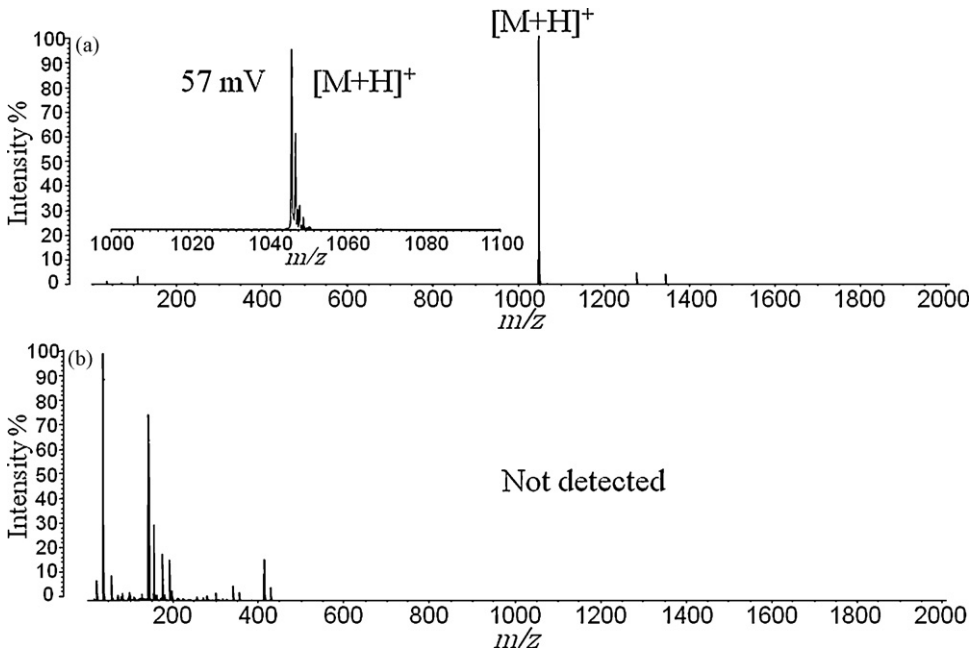

Fig. 3. SALDI mass spectra of angiotensin II (5 pmol) obtained using (a) a PGDS plate, and (b) a silicon plate from a deposition of Pt nanoparticle suspension as a SALDI matrix in a positive ion mode. The peak intensity is denoted by a unit of mV in the figure.

3.2. Surface-assisted laser desorption/ionization mass spectrometry (SALDI-MS) of peptides and small organic molecules using PGDS

Angiotensin II was chosen as a model peptide in the present study on SALDI performance using the PGDS plate because it is a typical peptide molecule, often used for the first screening of the ability of SALDI methods with regard to peptides. Fig. 2 shows the mass spectra of angiotensin II (5 pmol) obtained using the PGDS plate with immersing times of 5, 10, 30, and 60 min. As shown in Fig. 1, at a low Pt particle density at an immersing time of $t = 5$ min, peaks from angiotensin II were not observed in the mass spectrum. Using the Pt silicon plate at immersing times above 10 min, the peak intensity increased because of the increase in Pt particle density as shown in Fig. 1. At immersing times above 30 min, however, the unknown peaks became more pronounced in the low mass range of less than 400 m/z, which led to complication of the mass spectra. From the viewpoint of the peak intensity and the chemical background noises in the mass spectra, the PGDS plate with the 10-min immersion time was chosen for the SALDI-MS.

In a previous study, we reported that cationization by sodium and potassium was the dominant process in SALDI-MS using metal nanoparticles, irrespective of the presence of the typical TFA proton donor [34]. In this study, we found that protonated ions of angiotensin II tended to become dominant in the SALDI mass spectra using the PGDS plate, as shown in Fig. 3a. Only protonated ions of angiotensin II were observed in the mass spectrum. In contrast, the SALDI-MS using the silicon plate with the deposition of Pt nanoparticle suspension was not able to detect the peak of angiotensin II in the presence of TFA, as shown in Fig. 3b.

The above results indicate an increased number of protonated ions of peptides in SALDI-MS using a Pt-deposited silicon substrate. It has been suggested that near-surface hole-trapping results in a substantial increase in the acidity of surface Si–OH moieties, enabling proton transfer to hydrogen-bonded peptides with proton affinity [39,40]. According to this model, it is considered that platinum galvanic deposition on silicon with an n-Si/Pt Schottky barrier accelerates the near-surface hole trapping on the silicon surface because of a reduction in the recombination process of electron/hole pairs, causing an increase in the acidity of the Si–OH groups. The proton transfer from the Si–OH groups to the analyte molecules is enhanced, and finally, the thermal desorption of the analyte ions from the surface occurs, as reported by Alimpiev et al. [40]. It is likely that the Si–OH moieties originate from oxidation during its exposure to air prior to being inserted into the mass spectrometer. This is shown in the schematic diagram in Fig. 4.

3.3. Surface-assisted laser desorption/ionization mass spectrometry (SALDI-MS) of small organic molecules using PGDS

Because citrate buffer was not used in the SALDI-MS using PGDS, there are few chemical background ion peaks in the low mass region below 500 m/z. This results in the advantages of the matrix-free approach for small molecules. Fig. 5 shows the SALDI mass spectra of small molecules below 500 m/z, such as (a) caffeine and GGYR and (b) raffinose and β-cyclodextrin, obtained using the PGDS plate. For caffeine (195 m/z) and GGYR (452 m/z), only the protonated ions were observed in the mass spectra, while the molecule-related ions appeared as $[M+Na]^+$ for raffinose (527 m/z) and β-cyclodextrin (1157 m/z). The origin of the ions in the caffeine mass spectrum with masses greater than the $[M+H]^+$ peak is not clear at present. Deprotonation ions were observed in the mass spectrum for vita-

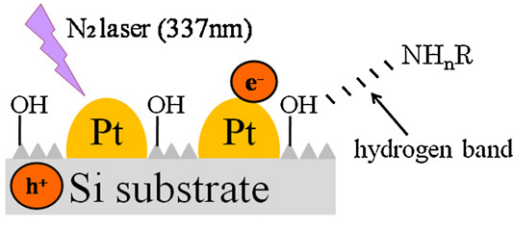

$$\equiv Si\text{-}OH\cdots NH_nR + h\nu \rightarrow \equiv Si^{+}\text{-}OH\cdots NH_nR + e^{-}$$

$$\equiv Si^{+}\text{-}OH\cdots NH_nR \rightarrow \equiv Si\text{-}O + H\text{-}N^{+}H_nR$$

Fig. 4. Schematic of UV radiation-mediated surface-localized positive charges from the effective charge separation (electron and hole) by PGDS plate, yielding the proton adduct form of peptides in SALDI-MS.

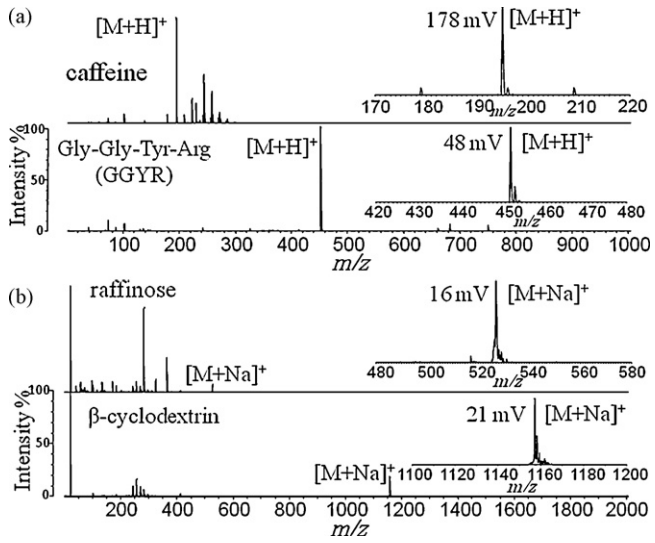

Fig. 5. SALDI mass spectra of (a) caffeine (100 pmol) and Gly-Gly-Tyr-Arg (5 pmol), and (b) raffinose (100 pmol) and β-cyclodextrin (100 pmol) in a positive ion mode.

min C in a negative ion mode, but the peaks from aspirin were not detectable even at 0.1 mM (Fig. 6). The detection limits of caffeine, raffinose, β-cyclodextrin, and vitamin C were 100 pmol. Thus, it is possible to detect these small molecules with SALDI-MS using the PGDS plate; however, the detection sensitivity of these small molecules remains an unresolved issue.

3.4. SALDI-MS of angiotensin II using evaporated Pt on silicon

In this study, we also examined the SALDI mass spectra of angiotensin II using evaporated Pt on oxidized silicon (plate A, n-Si/SiO_2/Pt contact) and evaporated Pt on bare silicon (plate B, n-Si/Pt contact), as shown in Fig. 7. The evaporated Pt on the bare silicon (plate B) substrate shows only protonated ions of peptides in the mass spectra, while the evaporated Pt on the oxidized silicon (plate A) substrate, where silicon oxides are clearly present between the silicon surface and the evaporated Pt, shows sodium and potassium adduct ions of the peptides besides the protonated ions. It seems that the direct contact of Pt particles with bare silicon is more effective in yielding protonated ions of peptides. In the case of evaporated Pt on oxidized silicon, which is prepared by UV/ozone irradiation, the thick silicon oxides on the silicon surface may inhibit the transformation of the laser photo-generated holes from n-silicon into the SiO_2 surface layer, resulting in an ineffective production of protonated ions of peptides. It should be noted that these analyte ions were generated from the evaporated Pt on silicon only with higher laser power, compared to the Pt galvanic deposition on silicon. As a result, the mass spectra were accompanied by a number of unknown signals in the low mass region (not shown).

3.5. SALDI-MS of angiotensin II using palladium galvanic deposition on silicon

Palladium, along with platinum, rhodium, ruthenium, iridium, and osmium, form a group of elements referred to as the platinum group metals. Platinum group metals share similar chemical properties. The SALDI performance for palladium (Pd) galvanic deposition on silicon was also investigated in this study. Fig. 8a shows the SEM image for Pd galvanic deposition on bare silicon with an immersing time of 10 min, which was the same reaction time as in the case of Pt. The SEM image shows 100–400 nm Pd particles on silicon. The mass spectrum of angiotensin II (5 pmol) obtained using Pd galvanic deposition on bare silicon is shown in Fig. 8b. Unexpectedly, cationization by sodium and potassium was the dominant process, irrespective of the presence of the typical TFA proton source. It is clear that platinum deposition on bare silicon is a good SALDI substrate for detection of peptides in the proton adducts form, while palladium galvanic deposition is not. The superior SALDI performance for Pt particles on silicon might have originated from close semiconductor–metal interface with good adhesion, such as in platinum silicides, which may be a necessary requirement for charge separation between Pt and silicon, leading to near-surface hole trapping in the silicon surface through a reduction in the electron/hole pair recombination process. Gorostiza et al. investigated the early stages of Pt galvanic deposition on Si(1 0 0) from HF solutions, and nucleations of polycrystalline platinum silicides were observed along with the etching of the substrate surface [36,41]. Thus, it is suggested that the UV irradiation surface-localized positive charges from the charge separation

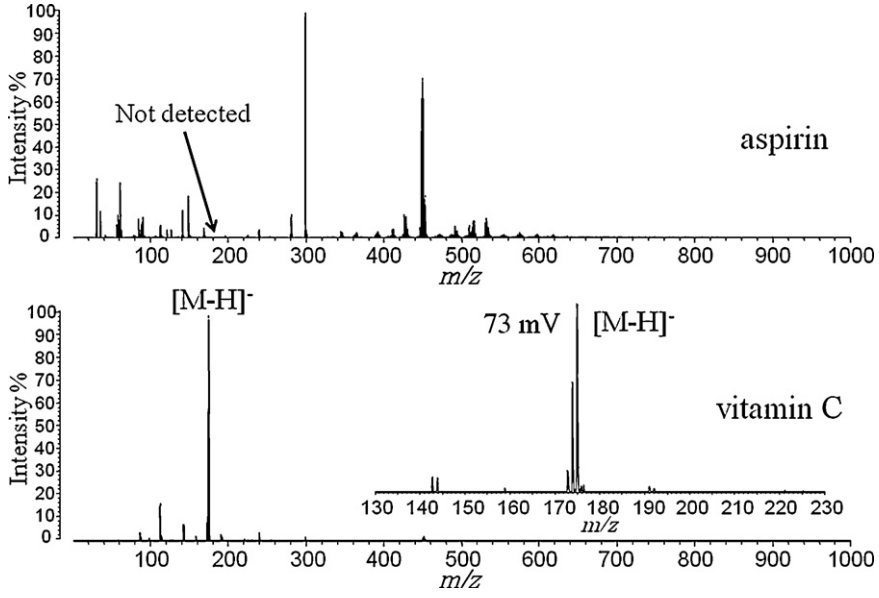

Fig. 6. SALDI mass spectra of aspirin (100 pmol) and vitamin C (100 pmol) in a negative ion mode.

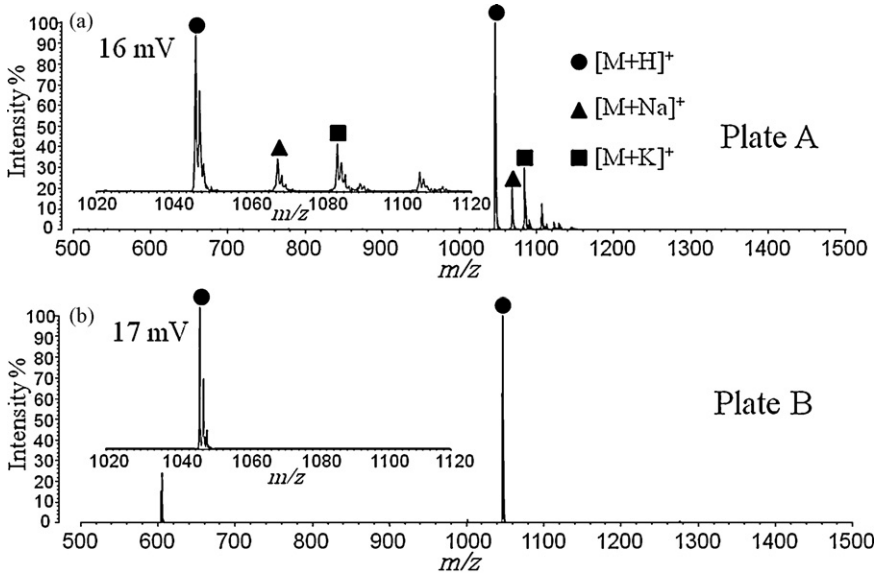

Fig. 7. SALDI mass spectra of angiotensin II (5 pmol) obtained using evaporated Pt on oxidized silicon (plate A) and evaporated Pt on bare silicon (plate B) in a positive ion mode.

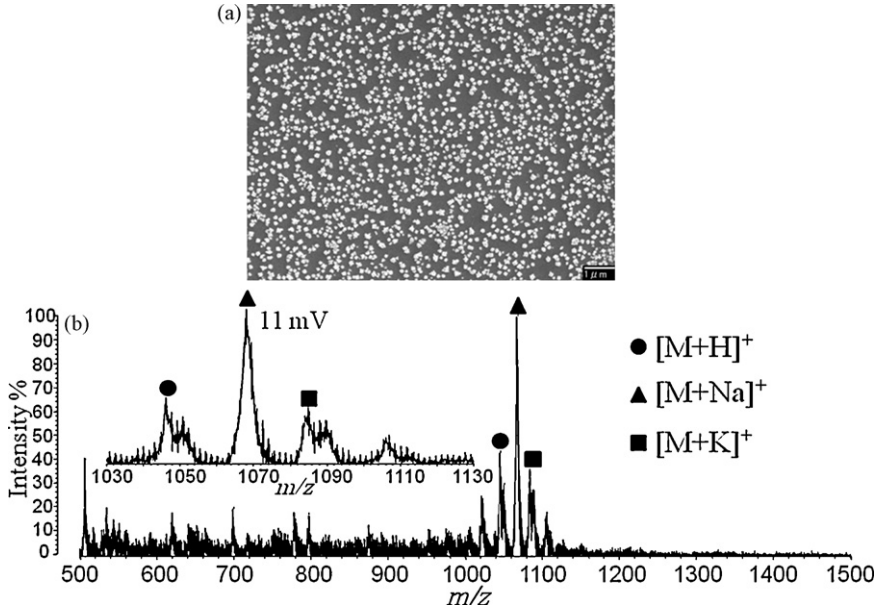

Fig. 8. (a) SEM image for the Pd particles on silicon, and (b) SALDI mass spectrum of angiotensin II (5 pmol) obtained using palladium galvanic deposition on silicon.

(electron and hole) in Pt particles on silicon surfaces are important to enable proton transfer to hydrogen-bonded peptides with proton affinity and to yield the proton adduct form of peptides in SALDI-MS.

4. Conclusion

The generation of peptide ions from Pt-deposited silicon substrates in surface-assisted laser desorption/ionization mass spectrometry (SALDI-MS) was studied using the following different SALDI substrates: (1) Pt galvanic deposition on silicon from HF solutions, (2) Pt nanoparticle deposition on silicon from the Pt particle suspension, (3) evaporated Pt on oxidized silicon, and (4) evaporated Pt on bare silicon. Among these substrates, the best substrate for SALDI was Pt galvanic deposition on silicon from HF solutions. Using this substrate, the proton adduct form of peptides was dominant in the SALDI mass spectra. In addition to platinum, palladium galvanic deposition was attempted as a SALDI-MS substrate, but was found to lead mainly to the Na^+ and K^+ forms of molecular ions. It was suggested that UV radiation-mediated surface-localized positive charges generated by charge separation (electron and hole) in Pt particles on silicon surfaces are important to effectively yield the proton adduct form of peptides in SALDI-MS. Semiconductors with Pt particle deposition may be useful for SALDI-MS of peptides because of the effective generation of UV radiation-mediated surface-localized positive charges.

Acknowledgements

This study was partially supported by a Grant-in-Aid for Scientific Research (B) and by Grant-in-Aid for Young Scientists (B) (No. 20710091 and 19350045) from the Japan Society for the Promotion of Science and the Ministry of Education, Culture, Sports, Science and Technology, Japan. This research was partly supported by the

Core-to-Core Program promoted by the Japan Society for the Promotion of Science (Project No. 18004). This study was supported by "Strategic Project to Support the Formation of Research Bases at Private Universities": Matching Fund Subsidy from MEXT (the Ministry of Education, Culture Sports, Science and Technology of Japan).

References

[1] M. Karas, F. Hillenkamp, Anal. Chem. 60 (1988) 2299.
[2] M.W.F. Nielen, Mass Spectrom. Rev. 18 (1999) 309.
[3] S.D. Hanton, Chem. Rev. 101 (2001) 527.
[4] K. Deisewerd, Chem. Rev. 103 (2003) 395.
[5] M. Karas, R. Kruger, Chem. Rev. 103 (2003) 427.
[6] R. Knochenmuss, R. Zenobi, Chem. Rev. 103 (2003) 441.
[7] F. Hillenkamp, J. Peter-Katalinic, MALDI-MS: A Practical Guide to Instrumentation, Methods and Applications, Wiley-Vch, 2007.
[8] J. Sunner, E. Dratz, Y.C. Chen, Anal. Chem. 67 (1995) 4335.
[9] S. Zumbuhl, R. Knochenmuss, S. Wulfert, F. Dubois, M.J. Dale, Anal. Chem. 70 (1998) 707.
[10] J. Kim, W. Kang, Bull. Korean Chem. Soc. 21 (2000) 401.
[11] Y.C. Chen, J.Y. Wu, Rapid Commun. Mass Spectrom. 15 (2001) 1899.
[12] T. Kinumi, T. Saisu, M. Takayama, H. Niwa, J. Mass Spectrom. 35 (2000) 417.
[13] M. Schulrenberg, K. Dreisewerd, F. Hillenkamp, Anal. Chem. 71 (1999) 221.
[14] R.A. Kruse, S.S. Rubakhin, E.V. Romanova, P.W. Bohn, J.V. Sweedler, J. Mass Spectrom. 36 (2001) 1317.
[15] K. Tanaka, H. Waki, Y. Ido, S. Akita, Y. Yoshida, T. Yoshida, Rapid Commun. Mass Spectrom. 2 (1988) 151.
[16] M.V. Ugarov, T. Egan, D.V. Khabashesku, J.A. Schultz, H. Peng, V.N. Khabashesku, H. Furutani, K.S. Prather, H.-W.J. Wang, S.N. Jackson, A.S. Woods, Anal. Chem. 76 (2004) 6734.
[17] T. Watanabe, H. Kawasaki, T. Yonezawa, R. Arakawa, J. Mass Spectrom. 43 (2008) 1063.
[18] C.T. Chen, Y.C. Chen, Anal. Chem 76 (2004) 1453.
[19] C.T. Chen, Y.C. Chen, Rapid Commun. Mass Spectrom. 18 (2004) 1956.
[20] C.T. Chen, Y.C. Chen, Anal. Chem. 77 (2005) 5912.
[21] H. Kawasaki, T. Yonezawa, T. Watanabe, R. Arakawa, J. Phys. Chem. C 111 (2007) 16278.
[22] J.A. Mclean, A.A. Stumpo, D.H. Russel, J. Am. Chem. Soc. 127 (2005) 5304.
[23] Y.F. Huang, H.T. Chang, Anal. Chem. 78 (2006) 1485.
[24] E.T. Castellama, D.H. Russel, Nano Lett. 7 (2007) 3023.
[25] H.-P. Wu, C.-L. Su, H.-C. Chang, W.-L. Tseng, Anal. Chem. 79 (2007) 6215.
[26] H. Kawasaki, T. Sugitani, T. Watanabe, T. Yonezawa, H. Moriwaki, R. Awakawa, Anal. Chem. 80 (2008) 7524.
[27] D.S. Stacy, J.D. Amaldo, K.R. William, S.C. Paul, H.R. David, Anal. Chem. 80 (2008) 6796.
[28] H. Yan, N. Xu, W.-Y. Huang, H.-M. Han, S.-J. Xiao, Int. J. Mass Spectrum. 281 (2009) 1.
[29] J. Wei, J.M. Buriak, G. Siuzdak, Nature 399 (1999) 243.
[30] Z. Shen, J.J. Thomas, C. Averbuj, K.M. Broo, M. Engelhard, J.E. Crowell, M.G. Finn, G. Siuzdak, Anal. Chem. 73 (2001) 612.
[31] S. Okuno, R. Arakawa, K. Okamoto, Y. Matsui, S. Seki, T. Kozawa, S. Tagawa, Y. Wada, Anal. Chem. 77 (2005) 5364.
[32] T. Seino, H. Sato, A. Yamamoto, A. Nemoto, M. Torimura, H. Tao, Anal. Chem. 79 (2007) 4827.
[33] D.S. Peterson, Mass Spectrom. Rev. 26 (2007) 19.
[34] T. Yonezawa, H. Kawasaki, A. Tarui, T. Watanabe, R. Arakawa, T. Shimada, F. Mafune, Anal. Sci. 25 (2009) 339.
[35] A. Tarui, H. Kawasaki, T. Taiko, T. Watanabe, T. Yonezawa, R. Arakawa, J. Nanosci. Nanotechnol. 9 (2009) 159.
[36] C. Carraro, R. Maboudian, L. Magagnin, Surf. Sci. Rep. 62 (2007) 499.
[37] S. Yae, N. Nasua, K. Matsumoto, T. Hagihara, N. Fukumuro, H. Matsuda, Electrochim. Acta 53 (2007) 35.
[38] I. Lombardi, S. Marchionna, G. Zangari, S. Pizzini, Langmuir 23 (2007) 12413.
[39] S. Alimpiev, S. Nikiforov, V. Karavansky, A. Grechnikov, J. Sunner, Proc. SPIE 5506 (2004) 95.
[40] S. Alimpiev, A. Grechnikov, J. Sunner, V. Karavansky, Y. Simanovsky, S. Zhabin, S. Nikiforov, J. Chem. Phys. 128 (2008) 014711.
[41] P. Gorostiza, R. Diaz, F. Sanz, J.R. Morante, J. Electrochem. Soc. 144 (1997) 4119.